GFD 2006 Lecture 5: Formation of mushy layers

Grae Worster; notes by Shane Keating and Ian Eisenman

March 15, 2007

1 Dissolution versus melting

In this lecture we will try to elucidate the difference between melting and dissolution of a solid in the presence of a two-component liquid mixture. We will consider pure solid ice at temperature $T_{-\infty} < T_m$ which is brought into contact with salt water that has a temperature higher than the liquidus temperature associated with its salt concentration C_0: $T_\infty > T_L(C_0)$.

The solution to this problem is very similar to a result from Lecture 4: the temperature and composition fields in the liquid and solid admit the similarity solution

$$T = \begin{cases} T_{-\infty} + (T_i - T_{-\infty}) \dfrac{\operatorname{erf}(\epsilon\eta)}{\operatorname{erf}(\epsilon\mu)} & \eta < \mu \quad \text{(ice)} \\ T_{-\infty} + (T_i - T_{-\infty}) \dfrac{\operatorname{erfc}(-\epsilon\eta)}{\operatorname{erfc}(-\epsilon\mu)} & \eta > \mu \quad \text{(liquid)} \end{cases}, \tag{1}$$

$$C = \begin{cases} 0 & \eta < \mu \quad \text{(ice)} \\ C_0 + (C_i - C_0) \dfrac{\operatorname{erfc}(\eta)}{\operatorname{erfc}(\mu)} & \eta > \mu \quad \text{(liquid)} \end{cases}, \tag{2}$$

$$\eta \equiv \frac{x}{2\sqrt{Dt}}, \tag{3}$$

$$\mu \equiv \frac{a}{2\sqrt{Dt}}. \tag{4}$$

The parameter $\epsilon \equiv \sqrt{D/\kappa}$ is assumed much less than unity. Rearranging (4), the interface location can be written as

$$a = 2\mu\sqrt{Dt}. \tag{5}$$

We seek the time evolution of the solid–liquid interface. From conservation of solute we have

$$C_i \dot{a} = -D \left(\frac{\partial C}{\partial x} \right)_{a_+}. \tag{6}$$

Substitution of (2) and (5) into (6) yields

$$C_i = \frac{C_0}{1 - F(\mu)}, \tag{7}$$

where $F(z) \equiv \sqrt{\pi} z e^{z^2} \mathrm{erfc}(z)$.

The initial concentration in the salt water is C_0, and as it is diluted by ablation of the ice, we expect $C_i < C_0$; hence $F(\mu)$ is negative. It is clear from Fig. 1 that this can only occur for negative values of μ. Thus $a(t)$ is receding in the negative x-direction and the picture of ice ablation causing reduced salt concentration near the interface is self-consistent.

The Stefan condition here is

$$\rho L \dot{a} = k \left[\frac{\partial T}{\partial x} \right]_{a^-}^{a^+}. \tag{8}$$

Plugging in (1) and (5) leads to

$$\sqrt{\frac{D}{\kappa}} \frac{L}{c_p} \mu = \frac{(T_i - T_{-\infty}) e^{-\epsilon^2 \mu^2}}{\sqrt{\pi} \mathrm{erfc}(-\epsilon\mu)} - \frac{(T_i - T_\infty) e^{-\epsilon^2 \mu^2}}{\sqrt{\pi} \mathrm{erfc}(\epsilon\mu)}. \tag{9}$$

We can simplify this result using the function $F(z)$:

$$\frac{L}{c_p} = \frac{T_i - T_\infty}{F(\epsilon\mu)} - \frac{T_i - T_{-\infty}}{F(-\epsilon\mu)}. \tag{10}$$

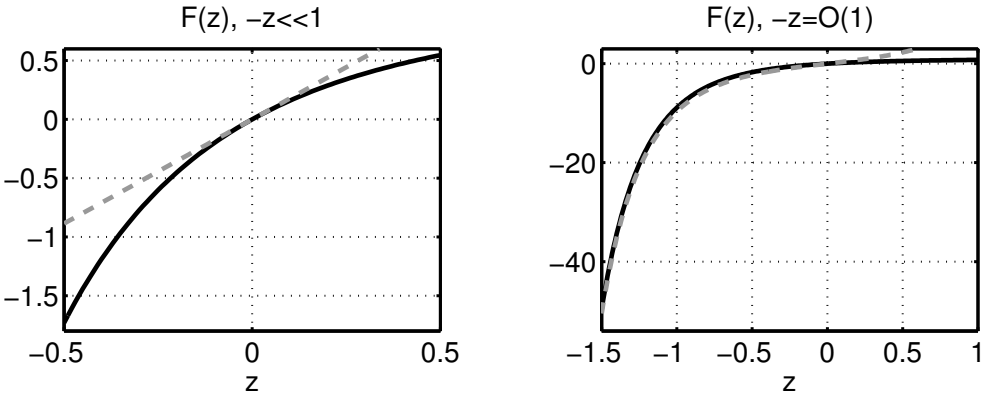

Figure 1: The function $F(z) \equiv \sqrt{\pi} z e^{z^2} \mathrm{erfc}(\mathrm{z})$ appearing in (7) and (10). The function is plotted in two different ranges of z, and approximations for $-z \ll 1$ and $-z \gg 1$ are indicated by gray dashed lines.

The similarity variable μ is unspecified at this point apart from its sign (μ is negative since we are considering ablation). In the following subsections, we will find two different mechanisms for the ablation of ice – dissolution and melting – which occur for different ranges of μ. A summary of the results of the remainder of this section is presented in Table (1).

1.1 Dissolution ($\mu = O(1)$)

Let us consider first the case where $\mu = O(1)$. For small z, the function $F(z) = \sqrt{\pi} z + O(z^2)$ (see Fig. 1), so that the Stefan condition (10) becomes

$$\frac{L}{c_p} = \left(\frac{T_i - T_\infty}{\sqrt{\pi}(\epsilon\mu)} - \frac{T_i - T_{-\infty}}{\sqrt{\pi}(-\epsilon\mu)} \right) (1 + O(\epsilon)). \tag{11}$$

	Dissolution	**Melting**
Parameter scaling	$-\mu = O(1)$	$-\mu = O\left(\epsilon^{-1}\right)$
Interface position	$a = O\left(\sqrt{Dt}\right)$	$a = O\left(\sqrt{\kappa t}\right)$
Interfacial temperature	$T_i < T_m$	$T_i \approx T_m$
Ablation limited by	Solute diffusion	Heat diffusion

Table 1: A comparison of the two different ablation mechanisms: dissolution and melting

Multiplying both sides by ϵ leads to

$$0 = \frac{T_i - T_\infty}{\sqrt{\pi}\mu} - \frac{T_i - T_{-\infty}}{\sqrt{\pi}\,(-\mu)} + O(\epsilon). \tag{12}$$

The interfacial temperature is thus approximately the mean of the far-field temperatures[1]:

$$T_i = \frac{1}{2}\left(T_\infty + T_{-\infty}\right) + O(\epsilon). \tag{13}$$

Since the interface temperature is assumed in equilibrium, it must lie on the liquidus, $T_i = T_L(C_i)$. The liquidus is a decreasing function of salt concentration (for concentration less than C_E), and concentration in the liquid at the interface is $C_i > 0$, so the solid–liquid interface is colder than the salt-free melting temperature, $T_i < T_m$. It is therefore clear that the interface temperature is too low to melt the ice simply by means of heat transfer: the ice requires the presence of the solute field to depress the local liquidus temperature sufficiently in order to change phase. This situation is depicted in Fig. 2.

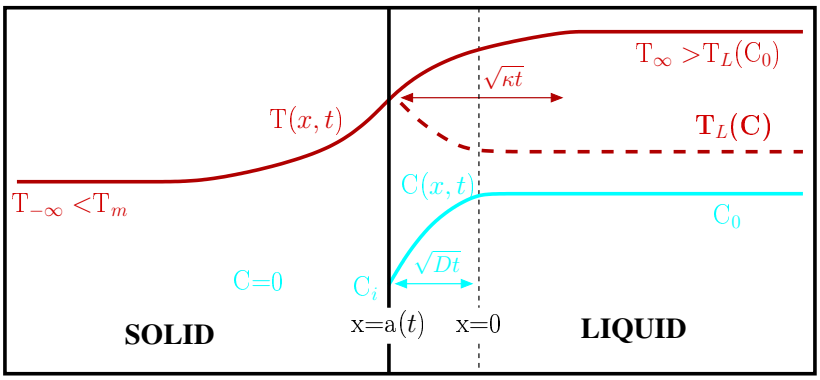

Figure 2: Dissolution of sea ice. Ablation rate is controlled by the transport of *salt* in the liquid.

As we can see from Fig. 2, the thickness of the melt layer $a(t)$ is of the same order as the thickness of the compositional boundary layer (Dt); this is indicated by the fact that

[1]Note that in Student Problem 4 the solid ice and liquid sea water were both at the same temperature ($T_{-\infty} = T_\infty$). In this situation, the interfacial temperature T_i is depressed below the far-field temperatures by an $O(\epsilon)$ correction, as implied by (12). It is this $O(\epsilon)$ term which we calculated.

$\mu = O(1)$. The rate of dissolution of the solid layer is limited by the rate at which we can supply salt to the interface: without enough solute, the liquidus temperature of the water adjacent to the interface will not be sufficiently below the actual temperature of the water and the solid ice cannot change phase. Thus, this is truly dissolution in the sense that the phase change from solid to liquid requires the presence of the salt field.

The phase diagram for this process of dissolution is shown in Fig. 3.

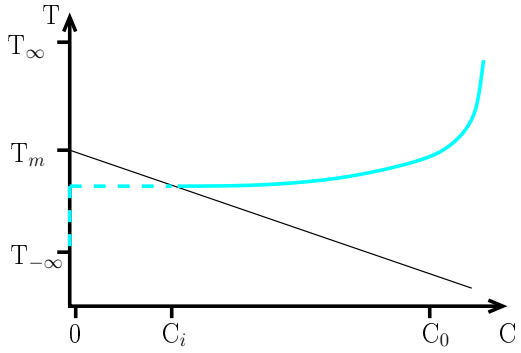

Figure 3: Phase diagram for dissolution. Solid curve represents the trajectory in temperature vs concentration space from the solid–liquid interface to the liquid far–field; continuation of trajectory on solid side of interface is indicated by dashed line. Diagonal line indicates liquidus.

In reality, gravity can play an important role in transporting solute to the interface via convection on a faster timescale than that given by diffusion alone. In the next lecture we will examine a situation incorporating convection.

1.2 Melting ($\mu = O(\epsilon^{-1})$)

For the case of $\mu \sim \epsilon^{-1}$ the interface will advance at a rate proportional to $\sqrt{\kappa t}$. In this situation, ablation of the ice is controlled by heat transfer. In contrast to the previous section, this is ablation caused by heating the material above the freezing temperature and hence is true melting. In the case of dissolution we used a small $-z$ approximation for $F(z)$ in (9); here, we will use a large $-z$ approximation for $F(z)$ in (7). For $-\mu \gg 1$, $\mathrm{erfc}(\mu) \approx 2$, and we have (see Fig. 1)

$$F(\mu) \approx -2\pi\mu e^{\mu^2} \qquad -\mu \gg 1. \tag{14}$$

Inserting this result, (7) becomes

$$C_i \approx \frac{C_0}{2\sqrt{\pi}\mu e^{\mu^2}}, \tag{15}$$

which approaches zero exponentially quickly as $|\mu| \to \infty$. Thus, the interface temperature is very close to the melting temperature of fresh water: $T_i = T_L(C_i) \approx T_L(0) = T_m$. As can be seen from Fig. 4, the interface recedes at a rate proportional to $\sqrt{\kappa t}$, leaving behind a salt-poor melt layer and a compositional boundary layer at $x = 0$. Note that the slope in the temperature field changes discontinuously as it moves through $x = a(t)$ due to the

release of latent heat. In the dissolution case this was an $O(\epsilon)$ effect, but here it can be quite significant.

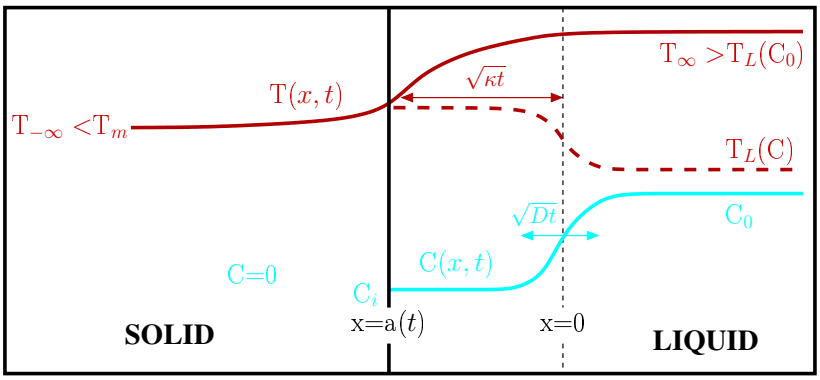

Figure 4: Melting of sea ice. Ablation rate is controlled by the transport of *heat* in the liquid.

The phase diagram for this scenario is depicted in Fig. 5. Note that no constitutional supercooling is possible during dissolution or melting of sea ice.

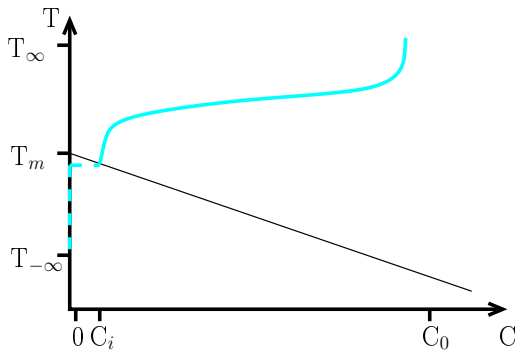

Figure 5: Phase diagram: as in Fig. 3, but for melting.

2 Mushy Layers

In Lecture 1, we saw that as a planar boundary solidifies into a supercooled melt, the interface is morphologically unstable to perturbations with a small but finite spatial wavelength. For the case of a binary melt, we saw in Lecture 4 that it was not necessary to supercool the liquid: differences in the rates of diffusion of heat and solute can give rise to a region where the actual temperature of the liquid is *less than the local liquidus temperature associated with the compositional field*. This phenomenon is known as *constitutional supercooling* and triggers morphological instability of the interface.

The evolution of the instability is depicted in cartoon form in Fig. 6. Initially small sinusoidal perturbations can be treated using weakly nonlinear analysis (which we do not consider here); it is observed that troughs narrow into crevasses while peaks become broader

and flatter. Experimental and numerical studies show that the instability proceeds via tip-splitting and side-branching until a matrix of fine dendritic crystals is formed. At this point, we must abandon all hope of following the exact solid–liquid interface and treat these crystals as a region of mixed phase: a so-called *mushy layer*. In the case of sea-ice, the crystals have a scale of about a millimeter; we are generally interested in scales of a meter or more, so it is appropriate to seek an averaged description of the mushy layer. We consider some arbitrary control volume containing representative elements of both solid and liquid, and we average over scales intermediate between the fine scale of the solid–liquid interface and the macroscopic scale of the sea-ice.

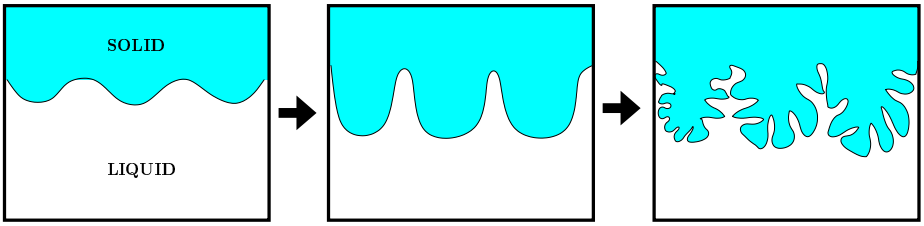

Figure 6: Evolution of the morphological instability

As we saw in the previous lecture, there are three natural lengthscales that characterize the morphological instability driven by constitutional supercooling: the thermal diffusion lengthscale is assumed much larger than either the solutal diffusion length or the capillary length. Thus, we may assume that the temperature field has enough time to relax to equilibrium between the solid and liquid phases within the mushy layer. The smallest scale, the capillary length, is much smaller than the mesoscale homogenization and details on this scale will be averaged out. Opinions differ, however, on whether the homogenization scale should be larger or smaller than the solutal diffusion lengthscale, and this, as we shall see, can impact the exact form of the field equations.

We seek an averaged description of the following fields:

- Mean temperature of the solid/liquid mixture $T(x,t)$,
- Concentration of the liquid phase $C(x,t)$,
- Volume fraction of the solid phase $\phi(x,t)$.

Averages will be taken over the control volume D bounded by surface δD and with unit normal $\mathbf{n}$ (Fig. 7).

We begin with conservation laws for this control volume. Here we will present only the calculation for conservation of mass. From continuity,

$$\frac{d}{dt}\int_D \bar{\rho} dV = -\int_{\delta D} \rho_l \mathbf{n}\cdot\mathbf{u} dS, \tag{16}$$

where $\bar{\rho}$ is the average density in the mushy layer,

$$\bar{\rho} = \rho_s\phi + (1-\phi)\rho_l. \tag{17}$$

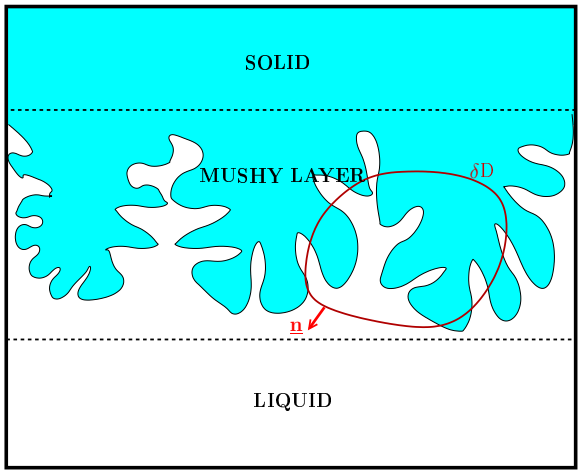

Figure 7: Control volume containing solid and liquid in a mushy layer.

Here the densities of the solid and liquid phases are ρ_s and ρ_l, respectively. We assume that the solid matrix is rigid and stationary[2] (although the ice can continue to grow), and that the only thing moving is the liquid. Thus, the mushy layer is a porous medium, and the velocity $\mathbf{u}$ in (16) is the *Darcy velocity*, or the mean volume flux of the liquid per unit area of the medium. The Darcy velocity is equal to the liquid volume fraction times the interstitial velocity, $u = (1-\phi)u_i$.

Averaging over the control volume D and applying the divergence theorem, (17) becomes

$$\int_D \left(\frac{\partial \bar{\rho}}{\partial t} + \nabla \cdot (\rho_l \mathbf{u}) \right) dV = 0. \tag{18}$$

Since (18) is true for an arbitrary control volume D, the integrand itself must be zero,

$$(\rho_s - \rho_l) \frac{\partial \phi}{\partial t} + \rho_l \nabla \cdot \mathbf{u} = 0, \tag{19}$$

where we have employed a Boussinesq approximation, assuming that the densities of liquid and solid phases are constant. Introducing the density ratio parameter $r \equiv \rho_s/\rho_l$, (19) can be rewritten as the divergence of a non-solenoidal velocity field,

$$\nabla \cdot \mathbf{u} = (1-r) \frac{\partial \phi}{\partial t}. \tag{20}$$

Thus, if the solid fraction ϕ is increasing (e.g., salt water is solidifying inside sea ice), then the fact that ice has a lower density than water means that the salt water will be squeezed out of the porous medium (we will neglect changes in density caused by salinity gradients). This phenomenon is known as *brine expulsion* in sea ice.

[2]When studying processes in large ice sheets, one might need to worry about compaction and deformation of the ice matrix. For example, fresh melt water beneath an ice shelf can depressurize and form ice crystals that "snow" upwards onto the bottom of the shelf. This layer can be compacted significantly, and in this case the matrix deformation cannot be neglected.

In a similar way, conservation of heat leads to

$$\overline{\rho c_p}\frac{\partial T}{\partial t} + \rho_l c_{pl}\mathbf{u}\cdot\nabla T = \nabla\cdot\left(\overline{k}\nabla T\right) + \rho_s L\frac{\partial \phi}{\partial t}. \tag{21}$$

Overbars represent mesoscale averaging. The gradient lengthscale of the temperature field is assumed much longer than the homogenization scale, and so is not averaged over. The average specific heat capacity is given by the exact expression

$$\overline{\rho c_p} = \phi\rho_s c_p + (1-\phi)\,\rho_l c_{pl}, \tag{22}$$

where c_{ps} and c_{pl} are the heat capacities of the solid and liquid phases.

The latent heat capacity is the difference in the enthalpies of the solid and liquid,

$$L(T,C) = H_l - H_s. \tag{23}$$

While L is in general a function of both T and C, we will assume that the mushy layer is in thermodynamic equilibrium, and hence the temperature field and the compositional field are linked by the liquidus relation. This allows us to write L as a function of only T or C.

The volume-averaged conductivity will, in general, be a function of the solid fraction, although what this functional dependence is depends upon the geometry of the mushy layer. For laminate layers, one can derive exact expressions for the conductivities: For the case where the heat flux is parallel to the laminar surfaces, the conductivity is

$$\overline{k} = k_{\parallel} = \phi k_s + (1-\phi)\,k_l \qquad \text{parallel heat flux,} \tag{24}$$

while for a perpendicular heat flux,

$$\overline{k} = k_{\perp} = \frac{1}{\phi/k_s + (1-\phi)/k_l} \qquad \text{perpendicular heat flux.} \tag{25}$$

It can be shown that for any porous medium the conductivity is bounded by the two laminar cases described above, so that

$$k_{\perp} \le \overline{k} \le k_{\parallel}, \tag{26}$$

as depicted in Fig. 8.

In the case of mushy layers in sea ice, the primary dendrites are plate-like and tend to align themselves with the prevailing temperature gradient: in this case, we shall take $\overline{k} = k_{\parallel}(\phi)$ to be a good approximation.

When considering the conservation of heat (21), the large separation of scales between the microscale and the thermal gradient length led to a robust averaging procedure. As mentioned earlier in this section, the separation of scales in the case of the solute field is less obvious. Thus, one representation of the solute conservation equation is (for liquidus/solidus distribution coefficient $k_D = 0$, as is approximately the case for sea-ice):

$$(1-\phi)\frac{\partial C}{\partial t} + \mathbf{u}\cdot\nabla C = \nabla\cdot\left(\bar{D}\nabla C\right) + rC\frac{\partial \phi}{\partial t}. \tag{27}$$

Ambiguity arises in the first term on the right-hand side of (27): by including it, we are implicitly assuming that the solutal diffusion lengthscale is larger than the homogenization

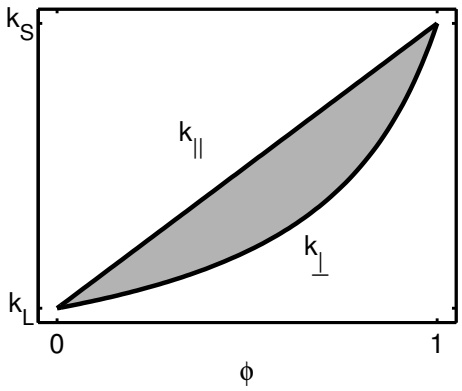

Figure 8: The conductivity of a porous medium is bounded by the laminar cases of parallel and perpendicular heat flux. The range of possible porous medium conductivities is indicated by the shaded region.

scale. If, on the other hand, the diffusion scale is comparable to or smaller than the scale on which we are taking volume averages, then this term vanishes. Indeed, the argument is related to where one draws the interface between the mushy layer and the liquid phase, which in turn raises questions about how one describes the mushy layer itself. In what follows, we shall scale out the offending term; however, it is worthwhile noting that this is a subject of ongoing investigation.

As in the case of the volume-averaged conductivity, the salt diffusivity takes the form

$$\bar{D} = D_l\,(1-\phi) = D_{\parallel}. \tag{28}$$

The final term in (27) describes the increase of the concentration in the interstitial region as the ice grows.

We further make the assumption that the mushy layer is in thermal equilibrium so that

$$T = T_L(C) \tag{29}$$

everywhere in the mushy layer. Hence the salt field and the thermal field are tied to one another inside the mushy layer by the liquidus curve, which precludes the possibility of any double-diffusive convection.

Finally, we require a transport equation for the liquid velocity $\mathbf{u}$. Since we are describing the mushy layer as a porous medium, it is appropriate to use Darcy's equation for flow through a porous medium:

$$\mu\mathbf{u} = \Pi\left(-\nabla P + \rho\mathbf{g}\right). \tag{30}$$

Here, μ is the kinematic viscosity, P is the pressure field, $\mathbf{g}$ is the gravitational acceleration, and Π is the permeability of the mushy layer. The latter will in general be a function of ϕ and geometry: we take it to be constant for simplicity. The introduction of the gravitational field introduces for the first time the possibilitity of convection, altering the heat flux from the liquid region (see later lectures, and Student Problem 5).

Equations (20), (21), (27), (29) and (30), along with the relevant boundary conditions and the equations for the liquid region, can be solved to obtain the temperature field,

concentration field, solid fraction and fluid velocity in the mushy layer in a frame of reference that is fixed with respect to the rigid stationary solid matrix. We consider solutions of these equations in the next lecture.

Student Problem 5: Effect of convection on melt rate for ice in pure water

Problem: Consider pure (i.e., salt-free) water with far-field temperature $T_\infty > T_m$ which is forced in an inviscid convective flow against ice at temperature $T = T_m = 0°\mathrm{C}$ (Fig. 9). Work in an axis system that moves with the ice edge, such that the ice-liquid interface is always at $z = 0$. In this frame, the water velocity field is

$$\mathbf{u} = (Ex, -Ez). \tag{31}$$

What is the melt rate V of the ice interface?

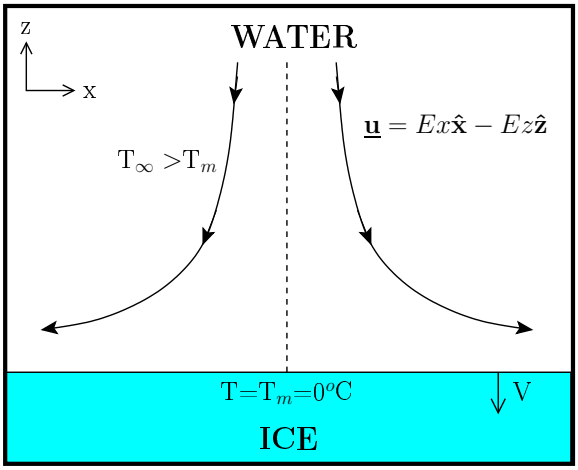

Figure 9: Student Problem 5. What is the melt velocity of the ice interface in the presence of convecting water?

Solution: We begin by seeking the temperature field in the water. In the moving axis system, T should be stationary in time; we also assume it is homogeneous in x. Introducing a dimensionless variable $\theta(z)$ to describe the z-dependence of the temperature field, we can write

$$T_\infty - T(z) = (T_\infty - T_m)\theta(z). \tag{32}$$

Equivalently,

$$T(z) = T_\infty - \Delta T\theta(z), \tag{33}$$

where we have defined $\Delta T \equiv T_\infty - T_m$. The water temperature boundary conditions are now

$$\theta(0) = 1 \quad , \tag{34}$$

$$\theta(z \to \infty) = 0. \tag{35}$$

The temperature field in the water satisfies the diffusion equation,

$$\frac{\partial T}{\partial t} + \mathbf{u} \cdot \nabla T = \kappa \nabla^2 T. \tag{36}$$

Inserting (33) and (31) into (36) yields

$$\theta''(z) = -\frac{Ez}{\kappa}\theta'(z). \tag{37}$$

The solution to (37) subject to (34) and (35) is, by analogy to similar differential equations solved in previous lectures,

$$\theta(z) = \operatorname{erfc}\left(\frac{z}{\lambda}\right), \tag{38}$$

with $\lambda \equiv \sqrt{\frac{2\kappa}{E}}$.

Given this temperature field we can find the interface velocity using the Stefan condition:

$$\rho L V = -k \left.\frac{\partial T}{\partial z}\right|_{0^+}. \tag{39}$$

The derivative of the temperature field from (33) and (38) is

$$\left.\frac{\partial T}{\partial z}\right|_{0^+} = -\Delta T \theta'(0) = \Delta T \frac{2}{\sqrt{\pi}\lambda}, \tag{40}$$

where we have used the definition of the erfc function to evaluate the derivative. Inserting (40), $k = \rho c_p \kappa$ (the definition of κ), the Stefan number $S \equiv L/\left(c_p \Delta T\right)$, and the definition of λ, we can solve (39) to get the interface velocity

$$V = -\frac{1}{S}\sqrt{\frac{2E\kappa}{\pi}}. \tag{41}$$

As in all examples, the ice melts faster if the Stefan number is small. We see here that the velocity of the melting interface depends on the square root of the convection velocity times the diffusion rate (as we might have guessed from dimensional analysis). The flow toward the phase boundary compresses the thermal boundary layer, which, by dimensional arguments, has thickness $\delta \sim \sqrt{\kappa/E}$. The compressed boundary layer leads to a steeper temperature gradient, thereby enhancing the heat flux from the liquid that causes melting.